Fluid Phase Equilibria 582 (2024) 114101

Contents lists available at ScienceDirect

Fluid Phase Equilibria

journal homepage: www.journals.elsevier.com/fluid-phase-equilibria

Solubility behavior and thermodynamic properties of caprolactam in four pure solvents and two cosolvent mixtures

Jianting Yang, Wen He, Meiqi Zhang, Jiangkun Hou, Shuanggen Wu, Xunqiu Wang *

School of Chemical Engineering, Zhengzhou University, Henan 450001, China

ARTICLE INFO

Keywords:
Caprolactam
Hansen solubility parameter
Solid-liquid equilibrium
Thermodynamic properties

ABSTRACT

The purpose of this work is to study the dissolution behavior of caprolactam in different solvents and to provide solid-liquid equilibrium data for the design and operation of crystallization and purification process for production and recovery of caprolactam. The mole fraction solubility of caprolactam was investigated in four pure solvents (benzene, ethyl acetate, cyclohexane, acetonitrile) and two cosolvent mixtures (ethyl acetate + cyclohexane, benzene + cyclohexane) by gravimetric method at atmospheric pressure from 277.65 K to 323.65 K. At the same temperature, the order of solubility of caprolactam in the selected pure solvents is: benzene > acetonitrile > ethyl acetate > cyclohexane. In the selected cosolvent mixtures, the solubility increases with increasing temperature and the content of good solvent. A series of thermodynamic models were used to fit the experimental solubility data. Finally, the thermodynamic properties of caprolactam in selected solvents were studied using the van't Hoff equation. From this analysis, it was concluded that the dissolution of caprolactam in the selected solvents is a heat-absorbing and entropy-increasing process.

1. Introduction

Caprolactam (molecular formula: $C_6H_{11}NO$; CAS number: 105602) is the monomer of nylon-6, an important organic chemical material used in the synthesis of polyamide fibers [1]. It is white flake crystal or crystalline powder at room temperature, greasy to the touch, hygroscopic, soluble in water and some organic solvents, such as methanol, ethanol, ether, acetone, and benzene. Nylon 6 is produced industrially by water-assisted ring-opening polymerization (ROP) of caprolactam with an annual production of 5 million tons. The market size of nylon-6 is increasing every year and is expected to reach $21.5 billion in 2026 [2]. Since nylon-6 fibers have unique physicochemical qualities, such as high impact resistance, flexibility, and exceptional tensile strength, they are widely employed in a variety of applications, including carpet, textile, coatings, automotive, and packing [3,4].

The purity of caprolactam greatly affects the mechanical and physical properties of nylon-6. As little as 0.1 % cyclohexanone oxime could drastically reduce the relative viscosity of the nylon-6 [5]. There are many industrial production processes of caprolactam [6,7], at present, the industrial production technology of caprolactam is mainly "ketone-oxime" process route [1], which accounts for about 95 % of the world's production of caprolactam. The core link is the transition of cyclohexanone and cyclohexanone oxime as intermediate products, and then through the Beckman rearrangement of cyclohexanone oxime, and then solvent extraction, distillation, ion exchange resin refining and other refining processes to produce caprolactam. The refining process of caprolactam is long and energy consuming. Therefore, refining caprolactam by crystallization has great advantages [8], such as reduced energy consumption and improved the purification efficiency. Solubility is a significant physicochemical characteristic for dissolving, crystallizing, and purifying materials. Therefore, knowing the precise solubility helps in optimizing the process operating conditions and designing the manufacturing process of the compound [9]. By studying the solubility of caprolactam in different solvents, suitable solvents for crystallization can be screened. Only two papers referring to the caprolactam solubility have been found [10,11]. However, there are no relevant reports regarding the solid-liquid equilibrium of caprolactam in cosolvent mixtures.

It is essential to determine the solubility data of caprolactam in additional solvents (pure solvents or cosolvent mixtures) in light of the above-described status quo. This effort aims to enhance its applicability in more routines. In this experimental investigation, the solubility of caprolactam in pure solvents (acetonitrile, ethyl acetate, benzene, cyclohexane) and two distinct cosolvent mixtures (ethyl acetate +

* Corresponding author.
E-mail address: zzusepaper@163.com (X. Wang).

https://doi.org/10.1016/j.fluid.2024.114101
Received 8 January 2024; Received in revised form 4 April 2024; Accepted 8 April 2024
Available online 9 April 2024

cyclohexane, and benzene + cyclohexane) was measured by gravimetric analysis at atmospheric pressure. Temperature control was maintained between 277.65 and 323.65 K in consideration of the fact that the experimental temperature in this investigation must not exceed the lowest boiling point (T_b) of the solvents employed and the melting point (T_m) of caprolactam. The modified Apelblat equation, the λh equation, the van't Hoff-Yaws model, and the NRTL model were utilized to correlate the caprolactam solubility data in four pure solvents. The modified Apelblat equation, the Apelblat-Sun equation, the van't Hoff-Yaws model and the NRTL model were additionally employed to correlate the solubility data in two cosolvent mixtures. Furthermore, the Hansen solubility parameter (HSP) was utilized as an explanation for the dissolution behavior of caprolactam. The thermodynamic properties of caprolactam in the given solvents were investigated by calculating the Gibbs energy, both the entropy and enthalpy of dissolution utilizing the van't Hoff equation. The results offer a thermodynamic foundation for the separation, crystallization, and purification of caprolactam.

2. Theoretical basis

2.1. Correlation models

The Modified Apelblat Equation [12,13], λh Equation [14], van't Hoff-Yaws model [15], NRTL Model [16,17] and Apelblat-Sun Equation [18–20] are used to correlate solubility data. The van't Hoff-Yaws model is as follows. Other models are listed in the support information.

The van't Hoff-Yaws model is a semi-empirical model, which could better reflect the relationship between solubility and temperature in different solvents. The expression is as follows:

$$\ln x_1 = A + \frac{B}{T/\mathrm{K}} + \frac{C}{(T/\mathrm{K})^2} \tag{1}$$

In the above equation, *A, B, C* stands for model parameters.

2.2. Hansen solubility parameter

Hansen solubility parameter (HSP) was introduced by C. Hansen [21] in 1967. HSP helps analyze the dissolution behavior of caprolactam in solvents. The total cohesive energy *E* of the liquid is divided into three distinct components based on intermolecular interaction forces, including dispersion interactions (E_d), polarity interactions (E_p) and hydrogen bonding interactions (E_h). Dispersion (δ_d), polarity (δ_p), and hydrogen bonding (δ_h) are the three partial solubility parameters of HSP. These values can be calculated using the following equations (2) and (3):

$$E = E_d + E_p + E_h \tag{2}$$

$$\frac{E}{V} = \frac{E_d}{V} + \frac{E_p}{V} + \frac{E_h}{V} \tag{3}$$

Where *V* denotes the molar volume, $\mathrm{L{\cdot}mol^{-1}}$, the total Hansen solubility parameter is described as follows (4):

$$(\delta_t)^2 = (\delta_d)^2 + (\delta_p)^2 + (\delta_h)^2 \tag{4}$$

For mixed solvents, the value of δ_M^{mix} can be determined using the following Eq. (5):

$$\delta_M^{mix} = \alpha\delta_M^1 + (1-\alpha)\delta_M^2 \text{ for M} = \mathrm{D,\ P,\ H} \tag{5}$$

Where δ_M^1 and δ_M^2 stand for the Hansen solubility parameters of mixed solvents; α stands for the volume fraction of a particular solvent in the mixed solvents. The values of δ_d, δ_P and δ_h are available in Hansen Solubility Parameters: a User's Handbook [22] or computed by the group contribution method proposed by Van Krevelen and Fedors [23–26], which can be expressed as follows (6)–(9):

Table 1
Information about the materials used in this experiment.

Chemicals reagents	CAS number	Molecular formula	Mass fraction purity	Source
Caprolactam	105–60–2	$C_6H_{11}NO$	≥0.995[a]	Shanghai Macklin Biochemical Co., Ltd
Acetonitrile	75–05–8	C_2H_3N	≥0.995[b]	Tianjin Kemi Chemical Reagent Co., Ltd
Ethyl acetate	141–78–6	$C_4H_8O_2$	≥0.995[b]	Tianjin Kemi Chemical Reagent Co., Ltd
Benzene	71–43–2	C_6H_6	≥0.995[b]	Shanghai Macklin Biochemical Co., Ltd
Cyclohexane	110–82–7	C_6H_{12}	≥0.995[b]	Tianjin Kemi Chemical Reagent Co., Ltd

[a] High-performance liquid chromatography, analyzed by the supplier.
[b] Gas chromatography, analyzed by the supplier.

$$\delta_D = \frac{\sum F_{d,i}}{V} \tag{6}$$

$$\delta_P = \frac{\sqrt{\sum F_{p,i}^2}}{V} \tag{7}$$

$$\delta_H = \sqrt{\frac{\sum E_{h,i}}{V}} \tag{8}$$

$$V = \frac{M}{\rho} \tag{9}$$

Where $F_{d,i}$, $F_{p,i}$, and $E_{h,i}$ show the contribution of group i to dispersion force, polar force, and hydrogen bond, respectively.

The miscibility of caprolactam and the solvents can be calculated based on the absolute value of the HSP difference $\Delta\delta_n$ and the comprehensive parameter $\Delta\delta$:

$$\Delta\delta_n = \left|\delta_{n,2} - \delta_{n,1}\right|,\ \mathrm{n = D,\ P,\ H,\ and\ t} \tag{10}$$

$$\Delta\delta = \left[(\delta_{H2} - \delta_{H1})^2 + (\delta_{P2} - \delta_{P1})^2 + (\delta_{D2} - \delta_{D1})^2\right]^{0.5} \tag{11}$$

2.3. Data correlation

In order to assess the fitting effect of each model, relative deviation (RD) (12), average relative deviation (ARD) (13), and root-mean-square deviation (RMSD) (14) were calculated.

Relative deviation (RD):

$$\mathrm{RD} = \frac{x_i^{exp} - x_i^{cal}}{x_i^{exp}} \tag{12}$$

Average relative deviation (ARD):

$$\mathrm{ARD} = \frac{\sum_{i=1}^{N}\left|\frac{x_i^{exp} - x_i^{cal}}{x_i^{exp}}\right|}{N} \tag{13}$$

Root mean square deviation (RMSD):

$$\mathrm{RMSD} = \sqrt{\frac{\sum_{i=1}^{N}\left(x_i^{exp} - x_i^{cal}\right)^2}{N}} \tag{14}$$

Where x_i^{cal} and x_i^{exp} are the calculated value and experimental solubility data of caprolactam, respectively; *N* indicates the number of the experimental points.

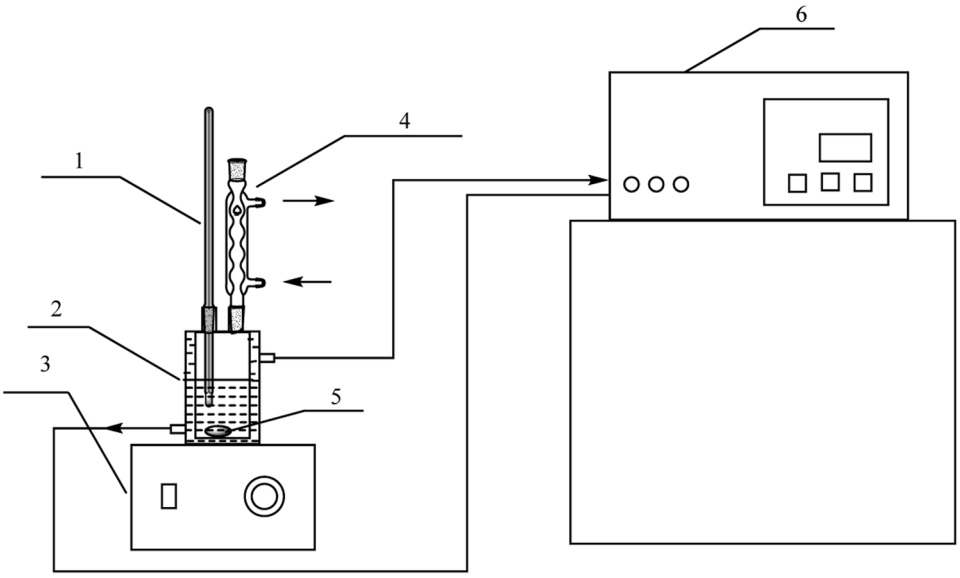

Fig. 1. Cartoon schematic of solubility measuring device.
1. Thermometer; 2. Dissolution kettle; 3. Magnetic stirrer; 4. Spherical condenser; 5. Magneton; 6. High-precision energy-saving thermostat bath.

3. Experimental section

3.1. Materials

Caprolactam with a purity exceeding 99.5 % (mass fraction) was procured from Shanghai Macklin Biochemical Co., Ltd. The details of chemicals utilized in this study are presented in Table 1. The chemicals were employed directly without subsequent purification.

3.2. Solubility determination

The solubility of caprolactam in pure solvents and cosolvent mixtures between 277.65 K and 323.65 K was investigated by gravimetric method (The device is shown in Fig. 1.). The accuracy of this experimental method and setup has been verified in our previous work [18–20, 27].

First, 50 mL of organic solvent and excess caprolactam were added to a 100 mL double-jacketed vessel, and the temperature in the vessel was controlled by circulating water from a high-precision energy-saving thermostat bath (GDH-2110, Ningbo Xinzhi Bio-technology Co., Ltd, Zhejiang, China, uncertainty ±0.05 K), and the temperature of the system is measured by a mercury thermometer (the uncertainty is ±0.05 K). And a magnetic stirrer with the agitation speed of 200 rpm was used to mix the suspension. The suspension was stirred continuously for 8 h at a specified temperature. This was done to ensure solid-liquid equilibrium. Stirring was stopped and the suspension was allowed to stand for at least 6 h to allow the insoluble matter to settle completely. After that, 3 mL of the supernatant was quickly drawn with a syringe and injected into a pre-weighed glass bottle. The glass bottle containing the sample was then immediately weighed on an analytical balance (BSA224S, Sartorius, Germany, with an accuracy of ±0.0001 g) and dried in a vacuum drying oven (DZF-6050,Shanghai Yiheng Scientific Instrument Co.Ltd.,China) at 323.15 K. When the difference between three consecutive weights is less than 0.0010 g, the mass was considered to be essentially constant. Three samples were repeatedly taken at each experimental point, and the solubility data were computed using the average value.

The solubility(x_1) in mole fraction of caprolactam can be expressed by an Eq. (15):

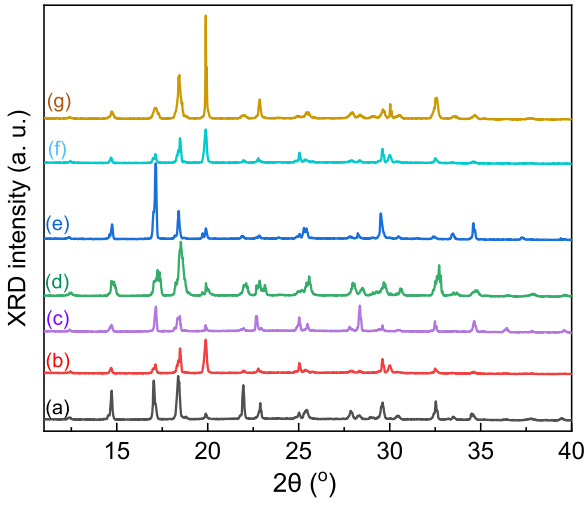

Fig. 2. PXRD patterns of samples. a Caprolactam raw materials; (b) Caprolactam + benzene; (c) Caprolactam + acetonitrile; (d) Caprolactam + cyclohexane; (e) Caprolactam + ethyl acetate; (f) Caprolactam + (benzene + cyclohexane); (g) Caprolactam + (ethyl acetate + cyclohexane).

$$x_1 = \frac{m_1/M_1}{m_1/M_1 + \sum_{j\neq 1}^{n} m_j/M_j} \tag{15}$$

Where m_1 and m_j stand for the mass of caprolactam and organic solvent, g, respectively; and M_1 and M_j denote their molar mass, g·mol^{-1}, respectively.

3.3. Powder X-ray diffraction (PXRD)

A powder X-ray diffractometer (D8 advance, Bruker, Germany, Cu-Kα radiation 0.15418) was utilized to determine whether caprolactam and saturated solution form a solid solvate or whether polycrystalline forms are present. Raw caprolactam and caprolactam recovered from different solvent systems were analyzed in the range of 2θ from 5° to 50° at a scan rate of 10 °min^{-1}.

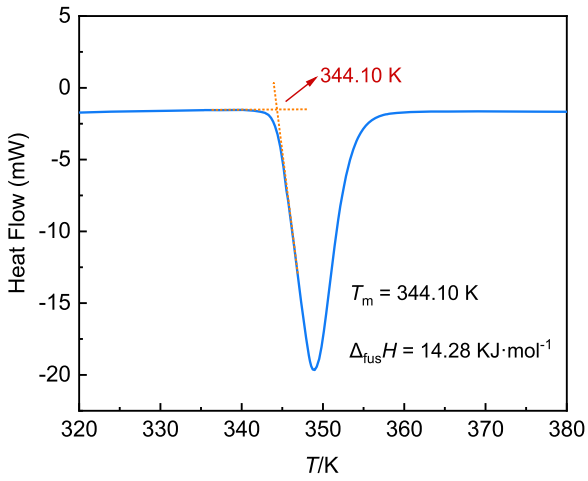

Fig. 3. DSC curve of caprolactam.

3.4. Thermal analysis (DSC)

Differential scanning calorimetry (DSC-60, Shimadzu, Japan) was utilized to analyze the melting characteristics of caprolactam, including the melting temperature (T_m) and enthalpy of fusion ($\Delta_{fus}H$). Indium and tin were used as standard substances, and the instrument was calibrated before measurement [18,28,29]. Then taken about 3.6 mg of caprolactam into an aluminum crucible, heating at a rate of 5 K·min^{-1} from 309.15 K to 393.15 K. The flow rate of N_2 was 50 mL·min^{-1}.

4. Results and discussion

4.1. PXRD results

After the solubility experiment, the PXRD curves of caprolactam and samples recovered in this study are shown in Fig. 2. No new diffraction peaks appear in the PXRD curves of the recovered caprolactam, as shown in Fig. 2, indicating that caprolactam has not undergone crystal form transformation during this work.

4.2. DSC results

Fig. 3 displays the DSC curve of caprolactam. There is only one single melting peak. The result shows that the melting temperature T_m of caprolactam is 344.10 K and the melting enthalpy $\Delta_{fus}H$ is 14.28 kJ·mol^{-1}.

Table 2
Experimental x_1^{exp} and calculatedx_1^{Cal} mole fraction solubility of caprolactam in four pure solvents from 277.65 K to 323.65 K under P = 101.325 kPa[a].

T/K	$100x_1^{exp}$	$100x_1{}^{Cal}$				100*RD*			
		Apelblat	λh	van't Hoff-Yaws	NRTL	Apelblat	λh	van't Hoff-Yaws	NRTL
Acetonitrile									
278.85	14.914	15.131	15.171	15.187	12.601	−1.46	−1.72	−1.83	15.51
283.65	18.709	19.112	19.093	19.197	15.909	−2.15	−2.05	−2.61	14.97
288.25	23.575	23.502	23.469	23.6	20.108	0.31	0.45	−0.11	14.70
293.55	29.391	29.251	29.26	29.356	25.638	0.48	0.45	0.12	12.77
298.45	35.93	35.193	35.286	35.265	31.866	2.05	1.79	1.85	11.31
303.65	42.688	42.094	42.296	42.136	38.844	1.39	0.92	1.29	9.01
308.15	48.561	48.493	48.77	48.515	45.201	0.14	−0.43	0.09	6.92
313.15	55.778	55.972	56.262	56.001	52.812	−0.35	−0.87	−0.40	5.32
318.65	63.675	64.507	64.667	64.616	61.309	−1.31	−1.56	−1.48	3.72
323.15	72.506	71.613	71.516	71.874	68.970	1.23	1.37	0.87	4.88
Ethyl acetate									
278.85	10.26	10.493	8.386	9.859	11.445	−2.27	18.27	3.91	11.55
283.65	12.651	12.994	11.339	12.524	14.133	−2.71	10.37	1.00	11.71
288.35	15.588	15.995	14.982	15.719	17.446	−2.61	3.89	−0.84	11.92
292.95	19.205	19.571	19.35	19.508	21.516	−1.91	−0.76	−1.58	12.03
298.05	24.347	24.435	25.178	24.609	27.213	−0.36	−3.41	−1.08	11.77
302.85	30.419	30.06	31.608	30.424	33.783	1.18	−3.91	−0.02	11.06
307.15	36.378	36.139	38.088	36.602	40.263	0.66	−4.70	−0.62	10.68
312.35	45.905	45.075	46.678	45.487	49.497	1.81	−1.68	0.91	7.83
317.15	55.709	55.178	55.122	55.268	58.258	0.95	1.05	0.79	4.58
321.55	65.364	66.32	63.073	65.762	66.122	−1.46	3.50	−0.61	1.16
Benzene									
279.25	19.976	20.510	18.787	19.617	18.244	−2.67	5.95	1.80	8.67
284.15	23.229	23.830	22.804	23.307	21.559	−2.59	1.83	−0.34	7.19
288.55	26.973	27.224	26.867	27.008	25.138	−0.93	0.39	−0.13	6.80
293.15	31.032	31.242	31.570	31.34	29.284	−0.68	−1.73	−0.99	5.63
297.85	36.093	35.903	36.836	36.332	34.240	0.53	−2.06	−0.66	5.14
303.05	42.309	41.796	43.157	42.413	40.396	1.21	−2.00	−0.25	4.52
307.25	48.168	47.190	48.591	47.839	45.985	2.03	−0.88	0.68	4.53
313.25	56.591	56.005	56.758	56.352	54.360	1.04	−0.30	0.42	3.94
317.45	63.112	63.047	62.678	63.017	60.609	0.10	0.69	0.15	3.97
321.75	70.075	71.089	68.837	70.313	67.149	−1.45	1.77	−0.34	4.18
Cyclohexane									
283.65	0.420	0.317	0.284	0.316	0.541	24.52	32.38	24.76	28.69
288.25	0.616	0.523	0.484	0.521	0.686	15.10	21.43	15.42	11.44
292.85	0.897	0.854	0.813	0.851	0.891	4.79	9.36	5.13	0.68
297.95	1.440	1.454	1.417	1.449	1.271	−0.97	1.60	−0.62	11.72
302.95	2.436	2.421	2.399	2.414	2.019	0.62	1.52	0.90	17.12
307.25	3.727	3.720	3.720	3.713	3.192	0.190	0.190	0.38	14.36
312.55	6.172	6.250	6.283	6.244	6.009	−1.26	−1.80	−1.17	2.63
318.35	10.843	10.884	10.924	10.883	12.946	−0.38	−0.75	−0.37	19.39
322.65	16.328	16.283	16.245	16.288	22.281	0.28	0.51	0.24	36.46

[a]Standard uncertainty u is $u(T)$ = 0.05 K, $u(P)$ = 0.3 kPa. The relative standard uncertainty is $u_r(x_1)$ = 0.05.

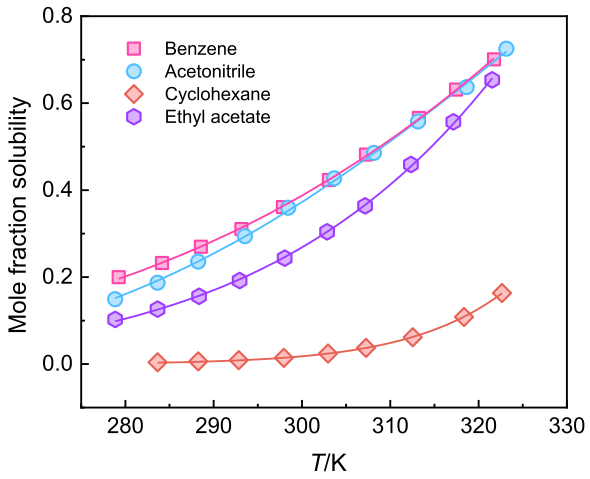

Fig. 4. Solubility of caprolactam in the pure solvents. Points represent experimental values; Lines are fitted values using van't Hoff-Yaws model.

4.3. Solubility data of caprolactam in four pure solvents

Firstly, the solubility data of caprolactam in acetonitrile, ethyl acetate, benzene and cyclohexane in the temperature range 277.65 K to 323.65 K was measured. The modified Apelblat equation, λh equation, van't Hoff-Yaws model and NRTL equation were applied to fit the solubility data and the results are presented in Table 2.

The modified Apelblat equation, the van't Hoff-Yaws model, the λh equation, and the NRTL model were employed for the correlation of the experimental solubility data. Origin 2022 software was used for data modeling. Table S1 presented the model parameters and the RAD, RMSD values. Among the four models, the average ARD are 2.33 % (Apelblat), 3.95 % (λh), 2.06 % (van't Hoff-Yaws), and 9.28 % (NRTL), respectively. And the average RMSD are 0.41 % (Apelblat), 0.66 % (λh), 0.27 % (van't Hoff-Yaws), and 2.24 % (NRTL), respectively. The results show that the minimum values of average ARD and RMSD are both observed in van't Hoff-Yaws model, indicating that this model can provide a favorable fitting effect. In addition, the unmeasured data points can be predicted using this model.

Table 3
Experimental x_1^{exp} and calculated x_1^{cal} mole fraction solubility of caprolactam (1) in ethyl acetate (2) + cyclohexane (3) from 277.65 K to 323.65 K under P = 101.325 kPa.[a].

T/K	$100x_1^{exp}$	$100x_1^{cal}$				$100RD$			
		Apelblat	Apelblat-Sun	van't Hoff-Yaws	NRTL	Apelblat	Apelblat-Sun	van't Hoff-Yaws	NRTL
w_2 = 20 %									
279.15	1.475	1.251	1.489	1.226	1.606	15.17	−0.97	16.88	−8.86
283.65	2.175	1.888	2.134	1.861	2.122	13.19	1.87	14.44	2.45
288.95	3.300	3.018	3.248	2.992	3.038	8.54	1.57	9.33	7.94
293.65	4.489	4.515	4.698	4.493	4.158	−0.59	−4.65	−0.09	7.38
298.15	6.718	6.567	6.669	6.553	6.338	2.25	0.73	2.46	5.66
303.65	10.327	10.233	10.193	10.237	10.386	0.91	1.30	0.87	−0.57
308.15	14.466	14.551	14.376	14.57	15.335	−0.58	0.62	−0.72	−6.00
313.75	21.727	22.254	21.966	22.289	23.774	−2.43	−1.10	−2.59	−9.42
318.75	32.289	32.141	31.955	32.168	33.962	0.46	1.04	0.37	−5.18
323.65	45.715	45.611	45.982	45.581	44.158	0.23	−0.58	0.29	3.41
w_2 = 40 %									
278.65	5.102	5.312	5.162	4.935	4.991	−4.12	−1.18	3.27	2.18
283.15	6.824	6.757	6.603	6.414	6.496	0.98	3.24	6.01	4.81
288.15	8.466	8.811	8.656	8.53	8.244	−4.08	−2.25	−0.76	2.62
292.85	10.964	11.287	11.137	11.087	10.782	−2.95	−1.58	−1.12	1.66
297.75	14.785	14.583	14.444	14.489	14.654	1.36	2.30	2.00	0.89
302.95	18.800	19.098	18.979	19.127	19.127	−1.59	−0.95	−1.74	−1.74
307.05	23.595	23.586	23.489	23.702	24.083	0.04	0.45	−0.45	−2.07
312.85	31.598	31.717	31.660	31.829	32.061	−0.38	−0.20	−0.73	−1.47
317.65	40.471	40.441	40.423	40.544	39.913	0.07	0.12	−0.18	1.38
322.45	51.446	51.466	51.487	51.284	48.530	−0.04	−0.08	0.31	5.67
w_2 = 60 %									
278.75	7.971	7.946	7.847	7.729	7.878	0.31	1.55	3.04	1.16
283.15	9.711	9.949	9.854	9.779	9.601	−2.46	−1.47	−0.70	1.13
288.15	12.662	12.741	12.654	12.637	12.370	−0.62	0.06	0.20	2.31
292.85	15.613	15.952	15.880	15.922	15.402	−2.17	−1.71	−1.98	1.35
297.75	19.901	20.016	19.964	20.065	19.662	−0.58	−0.32	−0.82	1.20
302.85	25.474	25.153	25.131	25.274	25.179	1.26	1.35	0.79	1.16
306.65	29.943	29.676	29.680	29.832	29.709	0.89	0.88	0.37	0.78
312.45	38.275	37.904	37.955	38.054	37.776	0.97	0.84	0.58	1.30
317.85	46.922	47.228	47.325	47.266	45.948	−0.65	−0.86	−0.73	2.08
322.45	56.560	56.632	56.769	56.451	54.060	−0.13	−0.37	0.19	4.42
w_2 = 80 %									
279.15	9.363	9.421	9.150	8.901	9.909	−0.62	2.28	4.93	−5.83
283.15	11.044	11.511	11.276	11.108	11.682	−4.23	−2.10	−0.58	−5.77
288.15	14.406	14.659	14.487	14.44	14.821	−1.76	−0.56	−0.24	−2.88
292.85	18.022	18.245	18.150	18.226	18.393	−1.24	−0.71	−1.13	−2.06
297.75	22.402	22.733	22.733	22.926	22.875	−1.48	−1.48	−2.34	−2.11
302.85	28.867	28.338	28.444	28.723	29.094	1.83	1.46	0.50	−0.78
307.15	34.525	33.907	34.099	34.393	34.786	1.79	1.23	0.38	−0.76
312.85	43.472	42.645	42.922	43.104	43.476	1.90	1.26	0.85	−0.01
317.85	51.834	51.747	52.046	51.948	51.574	0.17	−0.41	−0.22	0.50
322.45	61.044	61.458	61.701	61.138	59.792	−0.68	−1.08	−0.15	2.05

[a]Standard uncertainty u is $u(T)$ = 0.05 K, $u(P)$ = 0.3 kPa. The relative standard uncertainty is $u_r(x_1)$ = 0.05, u_r (w_2) = 0.0004, w_2 represents the mass fraction of ethyl acetate in the cosolvent mixture.

Table 4
Experimental x_1^{exp} and calculated x_1^{cal} mole fraction solubility of caprolactam (1) in benzene (2) + cyclohexane (3) from 277.65 K to 323.65 K under P = 101.325 kPa.[a].

T/K	$100x_1^{exp}$	$100x_1^{cal}$				100*RD*			
		Apelblat	Apelblat-Sun	van't Hoff-Yaws	NRTL	Apelblat	Apelblat-Sun	van't Hoff-Yaws	NRTL
w_2 = 20 %									
278.15	0.855	0.711	0.851	0.647	1.183	16.85	0.44	24.33	−38.40
284.15	1.480	1.314	1.469	1.235	1.658	11.24	0.75	16.55	−12.04
288.55	2.243	2.036	2.188	1.951	2.225	9.21	2.43	13.02	0.81
293.55	3.421	3.313	3.437	3.23	3.184	3.16	0.48	5.58	6.92
298.15	5.074	5.130	5.199	5.063	4.649	−1.11	2.47	0.22	8.38
303.55	8.566	8.469	8.433	8.444	8.041	1.13	1.55	1.42	6.13
308.15	12.748	12.852	12.709	12.879	12.627	−0.81	0.31	−1.03	0.95
313.65	20.852	20.918	20.704	21.008	21.704	−0.32	0.71	−0.75	−4.09
318.65	32.123	32.235	32.190	32.324	33.488	−0.35	0.21	−0.63	−4.25
323.35	48.084	47.986	48.637	47.906	48.084	0.20	1.15	0.37	0.00
w_2 = 40 %									
277.65	3.693	3.813	3.708	3.67	2.794	−3.24	0.41	0.62	24.34
283.45	5.685	5.723	5.624	5.595	4.663	−0.67	1.07	1.58	17.97
287.95	7.654	7.755	7.671	7.652	6.775	−1.32	0.22	0.03	11.49
292.65	10.416	10.545	10.486	10.482	9.926	−1.24	0.67	−0.63	4.71
298.15	14.875	14.923	14.907	14.923	15.106	−0.32	0.21	−0.32	−1.55
302.65	19.810	19.640	19.667	19.699	20.634	0.86	0.72	0.56	−4.16
307.25	25.720	25.790	25.860	25.903	27.006	−0.27	0.54	−0.71	−5.00
312.65	35.291	35.145	35.249	35.287	36.248	0.41	0.12	0.01	−2.71
317.25	45.640	45.367	45.461	45.469	45.441	0.60	0.39	0.37	0.44
322.75	60.806	60.971	60.959	60.88	58.269	−0.27	0.25	−0.12	4.17
w_2 = 60 %									
277.95	8.786	9.773	8.851	8.86	8.617	−11.23	0.74	−0.84	1.92
283.75	12.476	13.011	12.336	12.352	12.815	−4.29	1.12	0.99	−2.72
288.05	15.600	15.962	15.536	15.55	16.299	−2.32	0.41	0.32	−4.48
292.85	19.680	19.907	19.804	19.809	20.649	−1.15	0.63	−0.66	−4.93
298.15	25.334	25.186	25.455	25.441	26.210	0.58	0.48	−0.42	−3.46
302.65	31.220	30.547	31.087	31.053	31.600	2.15	0.43	0.53	−1.22
307.15	37.548	36.832	37.532	37.483	37.394	1.91	0.04	0.17	0.41
312.55	46.160	45.762	46.382	46.336	45.207	0.86	0.48	−0.38	2.06
317.15	54.989	54.724	54.902	54.899	52.944	0.48	0.16	0.16	3.72
322.25	65.515	66.310	65.409	65.526	62.337	−1.21	0.16	−0.02	4.85
w_2 = 80 %									
278.15	16.754	16.733	16.690	16.677	16.926	0.12	0.38	0.46	−1.02
283.95	20.444	20.654	20.627	20.622	20.641	−1.03	0.89	−0.87	−0.97
288.15	23.953	23.929	23.915	23.916	23.827	0.10	0.16	0.15	0.53
292.95	28.345	28.168	28.169	28.176	27.854	0.62	0.62	0.60	1.73
298.15	33.361	33.415	33.430	33.442	32.676	−0.16	0.21	−0.24	2.05
302.65	38.475	38.556	38.581	38.594	37.462	−0.21	0.28	−0.31	2.63
307.15	44.453	44.304	44.334	44.346	42.909	0.33	0.27	0.24	3.47
312.15	51.503	51.461	51.488	51.494	49.563	0.08	0.03	0.02	3.77
316.85	58.973	58.987	58.999	58.995	56.547	−0.02	0.04	−0.04	4.11
321.85	67.869	67.911	67.891	67.868	64.697	−0.06	0.03	0.00	4.67

[a]Standard uncertainty u is $u(T) = 0.05$ K, $u(P) = 0.3$ kPa. The relative standard uncertainty is $u_r(x_1) = 0.05$, $u_r(w_2) = 0.0004$, w_2 represents the mass fraction of benzene in the cosolvent mixture.

The solubility of caprolactam in the four pure solvents are shown in Fig. 4. When the temperature rises, caprolactam becomes more soluble in these solvents. The solubility of caprolactam in cyclohexane changes more slowly with increasing temperature up to 305 K. And the solubility increases significantly after 305 K. Fig. 4 demonstrated that, under identical temperature circumstances, the sequence of solubility (x_1^{exp}) in the selected pure solvents is benzene > acetonitrile > ethyl acetate > cyclohexane. The above solvents have the following polarity order: acetonitrile (46.0) > ethyl acetate (23.0) > benzene (11.1) > cyclohexane (0.6). The order of solubility is not exactly the same as the order of polarity. It is inferred that the polarity of the selected solvent is not a major factor affecting the solubility of caprolactam. Solubility is usually increased when molecules of the solvent and solute form hydrogen bonds. Because caprolactam has both a donor and an acceptor for hydrogen bonds on its molecule, it has a higher likelihood of forming hydrogen bonds with solvents. There is one hydrogen bond acceptor in the acetonitrile molecule, two in ethyl acetate, and neither a hydrogen bond acceptor or acceptor donor in cyclohexane. As a result, caprolactam is far more soluble in acetonitrile and ethyl acetate than in cyclohexane. Benzene lacks both donor and acceptor hydrogen bonds, although caprolactam dissolves readily in benzene. This is due to the fact that a number of variables, such as solvent polarity, intermolecular interactions, hydrogen bonding, and molecular structure [30], all affect solubility and should be further studied.

It is noted from the solubility measurement studies that caprolactam is soluble in acetonitrile, ethyl acetate and benzene. In contrast, its solubility in cyclohexane is significantly reduced. Consequently, ethyl acetate and benzene were selected as good solvents, and cyclohexane was selected as an anti-solvent, to assess caprolactam solubility in cosolvent mixtures (ethyl acetate + cyclohexane, benzene + cyclohexane). The results are crucial for directing the separation and purification of caprolactam.

4.4. Solubility data of caprolactam in two cosolvent mixtures

The solubility of caprolactam in two cosolvent mixtures (ethyl acetate + cyclohexane, benzene + cyclohexane) was determined from 277.65 K to 323.65 K. In this work, the experimental solubility data are fitted by four thermodynamic models: the modified Apelblat equation, Apelblat-Sun equation, van't Hoff-Yaws model and NRTL model.

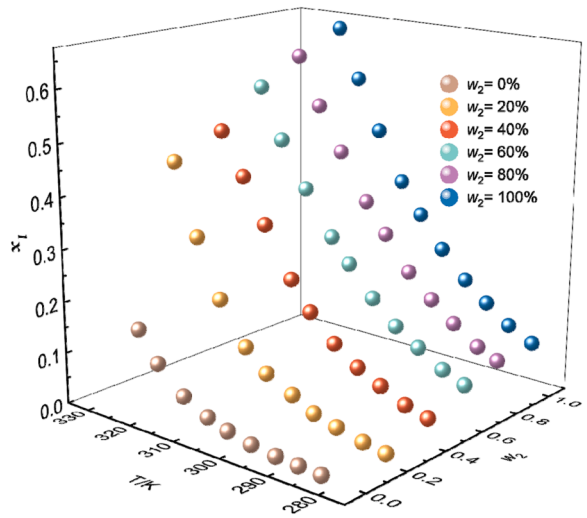

Fig. 5. Solubility of caprolactam in ethyl acetate (2) + cyclohexane (3) cosolvent mixture; Points represent experimental values; w_2 is the mass fraction of ethyl acetate in the cosolvent mixture.

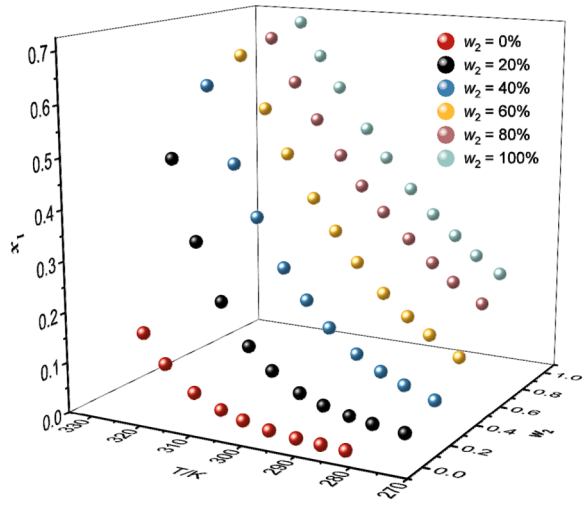

Fig. 6. Solubility of caprolactam in benzene 2 + cyclohexane 3 cosolvent mixture; Points represent experimental values; w_2 is the mass fraction of benzene in the cosolvent mixture.

Tables 3 and 4 display a summary of the experimental and calculated solubility values of caprolactam. Fig. 5 and Fig. 6 show the solubility data.

The experimental solubility data of caprolactam in the cosolvent mixtures were determined by the gravimetric method under normal pressure, and the data were fitted by four models mentioned above. Tables S2-S5 present the model parameters. The average ARD for four models is 2.10 % (Apelblat), 0.89 % (Apelblat-Sun), 2.02 % (van't Hoff-Yaws) and 4.09 % (NRTL), respectively. The average RMSD of three models is 0.26 % (Apelblat), 0.19 % (Apelblat-Sun), 0.18 % (van't Hoff-Yaws) and 1.04 % (NRTL), respectively. The calculated results indicate that the Apelblat-Sun equation and van't Hoff-Yaws model can achieve better fitting results.

It is evident from Fig. 5 and Fig. 6 that as temperature rises, caprolactam becomes more soluble in cosolvent mixtures. Meanwhile, the solubility of caprolactam increases with the rise in the mass fraction of co-solvents (ethyl acetate, benzene). The solubility of caprolactam in benzene (w_2 = 40 %) + cyclohexane system is less than that in ethyl acetate (w_2 = 40 %) + cyclohexane system, from 277.65 K to 298.15 K. However, the solubility of caprolactam in ethyl acetate (w_2 = 40 %) + cyclohexane system is less than that in benzene (w_2 = 40 %) + cyclohexane system in the temperature range (298.15 K − 322.75 K). The reason for this fluctuation is difficult to explain specifically because the solubility of caprolactam is affected by several conditions such as solute-solvent interactions, surface tension, and viscosity. Thus, more research is required to determine the precise causes.

4.5. Hansen solubility parameter

Table 5 displays the values of F_d, F_p and E_h for caprolactam. The HSP values for caprolactam and the used solvents are presented in Table 6. Typically, there is good mutual solubility when $\Delta\delta$ is less than 5.0 $MPa^{0.5}$ or less than 7.0 $MPa^{0.5}$ [31]. As can be seen from Table 6, the $\Delta\delta$ values of acetonitrile, benzene and cyclohexane are greater than 5 $MPa^{0.5}$, indicating that the solubility of caprolactam in these solvents should be relatively low. However, it is a fact that caprolactam has relatively high solubility in acetonitrile and benzene.

From Table 6, it can be found that benzene has the highest solubility for caprolactam, corresponding to the largest $\Delta\delta_D$, while cyclohexane has the lowest solubility for caprolactam, corresponding to the smallest δ_t. For pure solvents, the sequence of δ_t is acetonitrile > benzene > ethyl acetate > cyclohexane. The solubility sequence of caprolactam in pure solvents is benzene > acetonitrile > ethyl acetate > cyclohexane. There is no strict relationship between the order of solubility and the order of δ_t. Between caprolactam and four pure solvents, δ_D is similar, whereas δ_P and δ_H differ significantly. This suggests that the interaction between hydrogen bonding and polarity may greatly influence the solubility of caprolactam.

The δ_t values of the cosolvent mixtures are close to the δ_t of caprolactam. This implies that the $\Delta\delta_t$ value is small, indicating that caprolactam can easily dissolve in the two cosolvent mixtures chosen in this work. The values of $\Delta\delta_H$ and $\Delta\delta$ decrease accordingly as the mass fraction of co-solvent (benzene or ethyl acetate) in the cosolvent mixtures increases. In these systems (ethyl acetate + cyclohexane, benzene + cyclohexane), the minimum values of $\Delta\delta_H$ and $\Delta\delta$ were observed in ethyl acetate (w_2 = 80 %) + cyclohexane and benzene (w_2 = 80 %) + cyclohexane, and the solubility in each of the mixed systems reaches its maximum value at this time. In addition, the consistent trend of $\Delta\delta_H$ and $\Delta\delta$ means that the solubility of caprolactam in these systems (ethyl acetate + cyclohexane, benzene + cyclohexane) is mainly influenced by hydrogen bonding force.

4.6. Thermodynamic properties

The thermodynamic parameters of the dissolution process mainly include the standard enthalpy change of dissolution ($\Delta_{dis}H^0$), the standard entropy change of dissolution ($\Delta_{dis}S^0$), and the standard Gibbs free

Table 5
Group contribution table of caprolactam.

Group	Number	F_d ($J^{0.5}\bullet cm^{1.5}\bullet mol^{-1}$)	F_p ($J^{0.5}\bullet cm^{1.5}\bullet mol^{-1}$)	E_h ($J^{0.5}\bullet cm^{1.5}\bullet mol^{-1}$)
$-CH_2-$	5	270	0	0
-CO-	1	290	770	200
-NH-	1	160	210	3100

Table 6
Hansen solubility parameters of caprolactam and selected solvents.

Solvents	δ_D $(MPa)^{0.5}$	δ_P $(MPa)^{0.5}$	δ_H $(MPa)^{0.5}$	δ_t $(MPa)^{0.5}$	$\Delta\delta_D$ $(MPa)^{0.5}$	$\Delta\delta_P$ $(MPa)^{0.5}$	$\Delta\delta_H$ $(MPa)^{0.5}$	$\Delta\delta_t$ $(MPa)^{0.5}$	$\Delta\delta$ $(MPa)^{0.5}$
Acetonitrile	15.3	18.0	6.1	24.4	0.1	11.2	0.8	6.8	11.2
Ethyl acetate	15.8	5.3	7.2	18.2	0.4	1.5	1.9	0.6	2.5
Benzene	18.4	0.0	2.0	18.5	3.0	6.8	3.3	0.9	8.1
Cyclohexane	16.8	0.0	0.2	16.8	1.4	6.8	5.1	0.8	8.6
Caprolactam	15.4	6.8	5.3	17.6					
Ethyl acetate (w_2) + Cyclohexane									
w_2=0.2	16.6	0.9	1.4	17.0	1.2	5.9	3.9	0.6	7.1
w_2=0.4	16.4	1.9	2.8	17.3	1.0	4.9	2.5	0.3	5.6
w_2=0.6	16.2	3.0	4.2	17.6	0.8	3.8	1.1	0.0	4.1
w_2=0.8	16.0	4.1	5.6	17.8	0.6	2.7	0.3	0.2	2.8
Benzene (w_2) + Cyclohexane									
w_2=0.2	17.1	0.0	0.5	17.1	1.7	6.8	4.8	0.5	8.5
w_2=0.4	17.4	0.0	0.9	17.4	2.0	6.8	4.4	0.2	8.4
w_2=0.6	17.7	0.0	1.2	17.8	2.3	6.8	4.1	0.2	8.3
w_2=0.8	18.0	0.0	1.6	18.1	2.6	6.8	3.7	0.5	8.2

energy change ($\Delta_{dis}G^0$). These can be calculated by van't Hoff equation [9,32,33], that is calculated by the Eq. (16):

$$\ln x_1 = -\frac{\Delta_{dis}H^0}{R}\left(\frac{1}{T} - \frac{1}{T_{hm}}\right) - \frac{\Delta_{dis}G^0}{RT_{hm}} \quad (16)$$

The harmonic mean temperature T_{hm} can be calculated by Eq. (17):

$$T_{hm} = \frac{N}{\sum_{i=1}^{N}\frac{1}{T_i}} \quad (17)$$

N is the number of experimental points, $\Delta_{dis}H^0$, $\Delta_{dis}S^0$ and $\Delta_{dis}G^0$can be calculated by Eqs. (18)–(20) [34,35].

$$\Delta_{dis}H^0 = -R\left[\frac{\partial \ln x_1}{\partial(1/T - 1/T_{hm})}\right]_p = -R \times \text{slope} \quad (18)$$

$$\Delta_{dis}G^0 = -RT_{hm} \times \text{intercept} \quad (19)$$

$$\Delta_{dis}S^0 = \frac{(\Delta_{dis}H^0 - \Delta_{dis}G^0)}{T_{hm}} \quad (20)$$

Where T is the temperature of the solution, K.

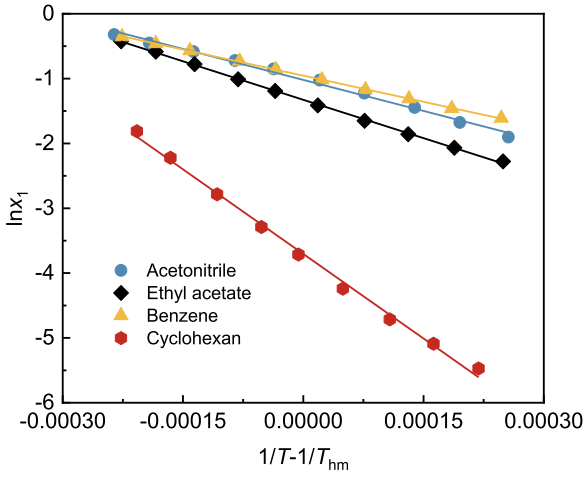

Fig. 7. $\ln x_1$ against $1/T\text{-}1/T_{hm}$ for caprolactam in four pure solvents.

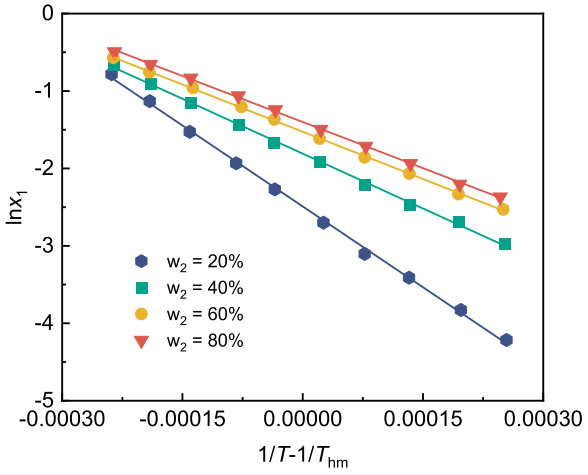

Fig. 8. $\ln x_1$ against $1/T\text{-}1/T_{hm}$ for caprolactam in a cosolvent mixture (ethyl acetate (w_2) + cyclohexane).

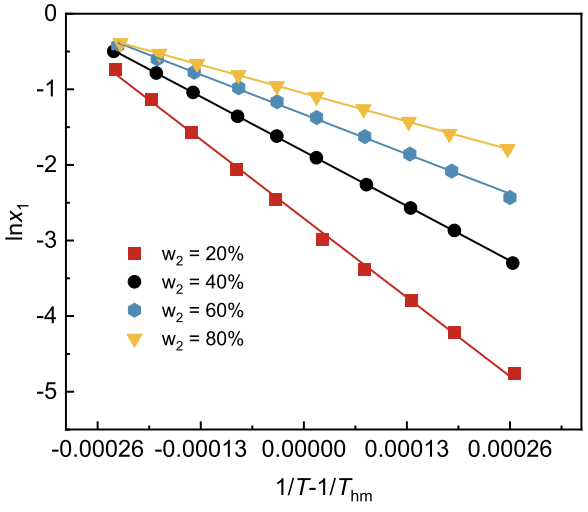

Fig. 9. $\ln x_1$ against $1/T\text{-}1/T_{hm}$ for caprolactam in a cosolvent mixture (benzene (w_2) + cyclohexane).

Table 7
Values of thermodynamic properties of caprolactam in four pure solvents and two cosolvent mixtures.

Solvent	$\Delta_{dis}H^0$ (kJ·mol^{-1})	$\Delta_{dis}G^0$ (kJ·mol^{-1})	$\Delta_{dis}S^0$ (J·K^{-1}·mol^{-1})	$10^2\xi_H$	$10^2\xi_{TS}$
Acetonitrile	26.52	2.55	79.82	52.52	47.48
Ethyl acetate	32.83	3.30	98.53	52.65	47.35
Benzene	22.34	2.38	66.56	52.81	47.19
Cyclohexane	72.34	9.31	208.41	53.44	46.56
Ethyl acetate (w_2) + cyclohexane, w_2=0.2	57.90	6.22	171.99	52.84	47.16
Ethyl acetate (w_2) + cyclohexane, w_2=0.4	39.24	4.51	115.89	53.05	46.95
Ethyl acetate (w_2) + cyclohexane, w_2=0.6	33.84	3.80	100.25	52.98	47.02
Ethyl acetate (w_2) + cyclohexane, w_2=0.8	32.99	3.49	98.41	52.79	47.34
Benzene (w_2) + cyclohexane, w_2=0.2	66.83	6.76	200.04	52.66	47.03
Benzene (w_2) + cyclohexane, w_2=0.4	46.25	4.53	139.24	52.58	47.42
Benzene (w_2) + cyclohexane, w_2=0.6	33.59	3.31	101.05	52.60	47.40
Benzene (w_2) + cyclohexane, w_2=0.8	23.90	2.62	71.04	52.90	47.10

[a]Standard uncertainty u, $u(\Delta_{dis}H^0) = 0.12$ kJ·mol^{-1}, $u(\Delta_{dis}G^0) = 0.05$ kJ·mol^{-1}, $u(\Delta_{dis}S^0) = 0.11$ J·K^{-1}·mol^{-1}.

The relative contribution of enthalpy (ξ_H) and entropy (ξ_{TS}) of the dissolution process is obtained by using Eqs. (21) and (22).

$$\xi_H = \frac{\left|\Delta_{dis}H^0\right|}{\left(\left|\Delta_{dis}H^0\right| + \left|T_{hm}\Delta_{dis}S^0\right|\right)} \quad (21)$$

$$\xi_{TS} = \frac{\left|T_{hm}\Delta_{dis}S^0\right|}{\left(\left|\Delta_{dis}H^0\right| + \left|T_{hm}\Delta_{dis}S^0\right|\right)} \quad (22)$$

$\ln x_1$ vs $(1/T - 1/T_{hm})$ in the four pure solvents and the two cosolvent mixtures are plotted in Figs. 7–9, respectively. By substituting the obtained intercept and slope into Eq. (18)–(20), $\Delta_{dis}H^0$, $\Delta_{dis}S^0$ and $\Delta_{dis}G^0$ can be calculated, ξ_H and ξ_{TS} can be obtained by Eqs. (21) and (22). Table 7 presents the calculated results.

The $\Delta_{dis}H^0$, $\Delta_{dis}G^0$, $\Delta_{dis}S^0$, ξ_H, ξ_{TS} values of caprolactam in solvents is given in Table 7. In Table 7, the values of $\Delta_{dis}G^0$ are positive, and $\Delta_{dis}G^0$ decrease as the mass fraction of cyclohexane decrease, reaching the maximum in cyclohexane. When the value of $\Delta_{dis}G^0$ is smaller, the solid-liquid equilibrium system is more stable. Less non-volumetric work is required for dissolution and the substance is more soluble in the system [9]. As shown in Table 7, the order of $\Delta_{dis}G^0$ is: cyclohexane > ethyl acetate > acetonitrile > benzene. This again indicates that caprolactam has maximum solubility in benzene and minimum solubility in cyclohexane. Besides, the values of $\Delta_{dis}H^0$ and $\Delta_{dis}S^0$ are positive, implying that the dissolution process is heat-absorbing and entropy-driven. Additionally, all ξ_H values are greater than ξ_{TS} and more than 52 %, indicating that the enthalpy is the main contributor to the standard Gibbs free energy in the dissolution process of caprolactam in selected solvents.

5. Conclusion

The solubility of caprolactam in selected solvents was studied through the gravimetric method at atmospheric pressure, covering the temperature range from 277.65 K to 323.65 K. The experimental result shows that the solubility of caprolactam increases gradually as temperature rises. Moreover, caprolactam exhibits its maximum solubility in benzene and minimum solubility in cyclohexane. Within cosolvent mixtures (ethyl acetate + cyclohexane, benzene + cyclohexane), caprolactam solubility increases as the mass fraction of the co-solvent (benzene, ethyl acetate) rises. In addition, the experimental solubility values of caprolactam were correlated with the modified Apelblat equation, λh equation, van't Hoff-Yaws model, NRTL model and Apelblat-Sun equation. Through deviation analysis, van't Hoff-Yaws model shows good fitting results to the solubility of caprolactam in the pure solvents, and the average ARD of the fitting is 2.06 %. The Apelblat-Sun equation and van't Hoff-Yaws model gave a good fit to the solubility data of caprolactam in the cosolvent mixtures used in this work, and the average ARD of the fitting is 0.89 %, 2.02 %, respectively. Furthermore, the solubility behavior of caprolactam was evaluated employing the Hansen solubility parameters. The solubility of caprolactam within cosolvent mixtures exhibits an inverse relationship with $\Delta\delta$.

Furthermore, we adopted the van't Hoff equation to calculated the thermodynamic properties. The positive values of $\Delta_{dis}H^0$, $\Delta_{dis}S^0$ and $\Delta_{dis}G^0$ show that the dissolution of caprolactam is a heat-absorbing, entropy-increasing process. ξ_H and ξ_{TS} were also calculated. The value of ξ_H is higher than that of ξ_{TS}, suggesting that the Gibbs free energy for caprolactam dissolution in selected solvents appears to be primarily influenced by enthalpy. This work provides insightful information for developing and enhancing the caprolactam crystallization process.

CRediT authorship contribution statement

Jianting Yang: Writing – review & editing, Writing – original draft, Software, Methodology, Investigation, Formal analysis, Data curation, Conceptualization. **Wen He:** Visualization, Validation, Software, Resources, Investigation, Data curation. **Meiqi Zhang:** Software, Resources, Investigation, Data curation. **Jiangkun Hou:** Writing – review & editing. **Shuanggen Wu:** Writing – review & editing, Conceptualization. **Xunqiu Wang:** Writing – review & editing, Supervision, Project administration, Funding acquisition, Conceptualization.

Declaration of competing interest

The authors declare that they have no known competing financial interests or personal relationships that could have appeared to influence the work reported in this paper

Data availability

Data will be made available on request.

Supplementary materials

Supplementary material associated with this article can be found, in the online version, at doi:10.1016/j.fluid.2024.114101.

References

[1] J. Ritz, H. Fuchs, H. Kieczka, W.C. Moran, Caprolactam, Ullmann's Encyclopedia of Industrial Chemistry, Wiley-VCH Verlag, Weinheim, Germany, 2011, https://doi.org/10.1002/14356007.a05_031.pub2.
[2] B. Herzog, M.I. Kohan, S.A. Mestemacher, R.U. Pagilagan, K. Redmond, R. Sarbandi, Ullmann's Encyclopedia of Industrial Chemistry, Wiley, Hoboken, 2000.
[3] L. Wursthorn, K. Beckett, J.O. Rothbaum, R.M. Cywar, C. Lincoln, Y. Kratish, T. J. Marks, Selective lanthanide-organic catalyzed depolymerization of Nylon-6 to

ϵ-Caprolactam, Angew. Chem. 135 (2023) 1–7, https://doi.org/10.1002/ange.202212543.
[4] B. Deopura, R. Alagirusamy, M. Joshi, B. Gupta, Polyesters and Polyamides, Elsevier, Amsterdam, 2008.
[5] L.T. Fisyuk, L.A. Lezhnina, V.T. Butkin, The influence of impurities in the caprolactam on the properties of the polycaproamide, Fibre Chem. 10 (1978) 3–5, https://doi.org/10.1007/BF00545924.
[6] E.A. Martynenko, I.L. Glazko, S.V. Levanova, Cyclohexanone in the production of caprolactam. Problems and solutions, Russ. Chem. Bull. 65 (2016) 2513–2521, https://doi.org/10.1007/s11172-016-1616-4.
[7] G.B. Gechele, G. Stea, F. Manescalchi, Cationic polymerization of caprolactam, Eur. Polym. J. 4 (1968) 505–513, https://doi.org/10.1016/0014-3057(68)90069-4.
[8] J. Synowiec, P. Synowiec, Industrial purification of caprolactam by means of crystallization from aqueous solution, Cryst. Res. Technol. 18 (1983) 951–957, https://doi.org/10.1002/crat.2170180720.
[9] E. Choi, P.M. Heynderickx, Solubility measurement and correlation of 2-amino-terephthalic acid in eight alcoholic solvents at different temperatures, J. Chem. Thermodyn. 177 (2023) 106948, https://doi.org/10.1016/j.jct.2022.106948.
[10] C. Guo, L. Li, J. Cheng, J. Zhang, W. Li, Solubility of caprolactam in different organic solvents, fluid phase equilib. 319 (2012) 9–15. doi:10.1016/j.fluid.2011.12.004.
[11] S. Guo, W. Su, H. Hao, Y. Luan, X. Li, S. Gao, X. Huang, Solution thermodynamics of caprolactam in different monosolvents, J. Chem. Eng. Data. 66 (2021) 494–503, https://doi.org/10.1021/acs.jced.0c00741.
[12] A. Apelblat, E. Manzurola, Solubilities of o-acetylsalicylic, 4-aminosalicylic, 3,5-dinitrosalicylic, and p-toluic acid, and magnesium-DL-aspartate in water from T = (278 to 348) K, J. Chem. Thermodyn. 31 (1999) 85–91, https://doi.org/10.1006/jcht.1998.0424.
[13] A. Apelblat, E. Manzurola, Solubilities of L-aspartic, DL-aspartic, DL-glutamic, p-hydroxybenzoic, o-anisic, p-anisic, and itaconic acids in water from T = 278 K to T = 345 K, J. Chem. Thermodyn. 29 (1997) 1527–1533, https://doi.org/10.1006/jcht.1997.0267.
[14] H. Buchowski, A. Ksiazczak, S. Pietrzyk, Solvent activity along a saturation line and solubility of hydrogen-bonding solids, J. Phys. Chem. 84 (1980) 975–979, https://doi.org/10.1021/j100446a008.
[15] P. Cysewski, T. Jeliński, D. Procek, A. Dratwa, Solubility of sulfanilamide and sulfacetamide in neat solvents: measurements and interpretation using theoretical predictive models, first principle approach and artificial neural networks, Fluid Phase Equilibr. 529 (2021) 112883, https://doi.org/10.1016/j.fluid.2020.112883.
[16] H. Renon, J.M. Prausnitz, Estimation of parameters for the NRTL equation for excess gibbs energies of strongly nonideal liquid mixtures, Ind. Eng. Chem. Proc. Des. Dev. 8 (1969) 413–419, https://doi.org/10.1021/i260031a019.
[17] H. Renon, J.M. Prausnitz, Local composition thermodynamic excess functions for liquid mixtures, AIChE J. 14 (1968) 135–144, https://doi.org/10.1002/aic.690140124.
[18] S. Xue, J. Chu, H. Yin, X. Wang, Study on the solid-liquid equilibrium of triphenylphosphine in four mono-solvents and two mixed solvents, J. Chem. Thermodyn. 176 (2023) 106910, https://doi.org/10.1016/j.jct.2022.106910.
[19] Z. Gao, Y. Li, X. Wang, Study on the solid-liquid equilibrium of L-malic acid in binary solvents, J. Mol. Liq. 325 (2021) 115113, https://doi.org/10.1016/j.molliq.2020.115113.
[20] L. Zhang, Y. Zuo, H. Liu, X. Wang, Study on the solid-liquid equilibrium of bifenthrin in solvents, J. Mol. Liq. 308 (2020) 113033, https://doi.org/10.1016/j.molliq.2020.113033.
[21] C.M. Hansen, The three-dimensional solubility parameter-key to paint component affinities. I. solvents, plasticizers, polymers, and resins, J. Paint Technol. 39 (1967) 104–117.
[22] C.M. Hansen, Hansen Solubility Parameters: A UserS Handbook, 2nd edition, CRC Press, Boca Raton, London, New York, 2007.
[23] D.L. Williams, K.D. Kuklenz, A determination of the hansen solubility parameters of Hexanitrostilbene (HNS), Propellants Explos. Pyrotech. 34 (2009) 452–457, https://doi.org/10.1002/prep.200800045.
[24] D.W. Van Krevelen, K.T. Nijenhuis, Properties of Polymers, Elsevier, Amsterdam, 2009 four edition.
[25] R.F. Fedors, A method for estimating both the solubility parameters and molar volumes of liquids, Polym. Eng. Sci. 14 (1974) 147–154, https://doi.org/10.1002/pen.760140211.
[26] S. Just, F. Sievert, M. Thommes, J. Breitkreutz, Improved group contribution parameter set for the application of solubility parameters to melt extrusion, Eur. J. Pharm. Biopharm. 85 (2013) 1191–1199, https://doi.org/10.1016/j.ejpb.2013.04.006.
[27] J. Lu, H. Chen, Y. Huang, L. Zhang, Z. Zhao, W. Du, X. Wang, Thermodynamic equilibrium of hexamethylenediammonium glutarate in mono-solvents and binary solvent systems, Fluid Phase Equilib. 485 (2019) 1–15, https://doi.org/10.1016/j.fluid.2018.12.008.
[28] S.M. Sarge, E. Gmelin, G.W.H. Höhne, H.K. Cammenga, W. Hemminger, W. Eysel, The caloric calibration of scanning calorimeters, Thermochim. Acta 247 (1994) 129–168, https://doi.org/10.1016/0040-6031(94)80118-5.
[29] R. Sabbah, An Xu-wu, J.S. Chickos, M.L. Planas Leitão, M.V. Roux, L.A. Torres, Reference materials for calorimetry and differential thermal analysis, Thermochim. Acta 331 (1999) 93–204, https://doi.org/10.1016/S0040-6031(99)00009-X.
[30] M. Zheng, J. Chen, G. Chen, A. Farajtabar, H. Zhao, Solubility modelling and solvent effect for domperidone in twelve green solvents, J. Mol. Liq. 261 (2018) 50–56, https://doi.org/10.1016/j.molliq.2018.03.121.
[31] M.A. Mohammad, A. Alhalaweh, S.P. Velaga, Hansen solubility parameter as a tool to predict cocrystal formation, Int. J. Pharm. 407 (2011) 63–71, https://doi.org/10.1016/j.ijpharm.2011.01.030.
[32] R.R. Krug, W.G. Hunter, R.A. Grieger, Enthalpy-entropy compensation. 1. Some fundamental statistical problems associated with the analysis of van't Hoff and Arrhenius data, J. Phys. Chem. C 80 (1976) 2335–2341, https://doi.org/10.1021/J100562A006.
[33] R.R. Krug, W.G. Hunter, R.A. Grieger, Enthalpy-entropy compensation. 2. Separation of the chemical from the statistical effect, J. Phys. Chem. C 80 (1976) 2341–2351, https://doi.org/10.1021/j100562a007.
[34] M.A. Parra, N.E. Cerquera, C.P. Ortiz, R.E. Cárdenas-Torres, D.R. Delgado, M.Á. Peña, F. Martínez, Solubility of ciprofloxacin in different solvents at several temperatures: measurement, correlation, thermodynamics and Hansen solubility parameters, J. Taiwan Inst. Chem. Eng. 150 (2023) 105028, https://doi.org/10.1016/j.jtice.2023.105028.
[35] F. Li, Y. Chen, Y. Li, Y. Wan, X. Gao, J. Xiao, S. Ma, Y. Yu, 2,3-Dichloropyridine solubility in 14 pure solvents: determination, correlation, Hansen solubility parameter, solvent effect and thermodynamic analysis, J. Chem. Thermodyn. 191 (2024) 107229, https://doi.org/10.1016/j.jct.2023.107229.